Does the Onset of Water Droplet Formation Alter the Microenvironment of the Hydrophobic Probes Solubilized in Nonionic Reverse Micelles?

G. B. Dutt*

Radiation Chemistry and Chemical Dynamics Division, Bhabha Atomic Research Centre, Trombay, Mumbai 400 085, India

Received: February 25, 2004; In Final Form: March 31, 2004

The interiors of the reverse micelles formed with the surfactant Triton X-100 (TX-100) in benzene−*n*-hexane mixed solvent with an increasing water content, $W = [H_2O]/[TX\text{-}100]$, have been explored by monitoring the fluorescence anisotropies of two structurally similar but chemically distinct hydrophobic probes. The objective of this work is to find out how the formation of the water pool influences the location and mobility of these probe molecules. It has been observed that the anisotropies of both the probes 2,5-dimethyl-1,4-dioxo-3,6-diphenylpyrrolo[3,4-*c*]pyrrole (DMDPP) and 1,4-dioxo-3,6-diphenylpyrrolo[3,4-*c*]pyrrole (DPP) decay as a sum of two exponentials with slow and fast time constants. This experimental finding has been rationalized on the basis of a two-step model according to which the probe molecule undergoes two different kinds of motion inside the micelle. The average reorientation times of DPP are a factor of 4 longer than that of DMDPP. This observation in conjunction with the fact that the order parameters of both the probes are considerably different from one another indicates that DMDPP and DPP are located in different regions of the core of the reverse micelles. Another significant observation is that there is no variation in the average reorientation times of both DMDPP and DPP with W once the water pool formation takes place in these reverse micelles. This result implies that the respective microenvironments experienced by the probes essentially remain the same with the onset of water droplet formation.

1. Introduction

Reverse micelles are a class of molecular assemblies whose interiors are comprised of the polar headgroups of the amphiphiles that form the aggregates and are surrounded by nonpolar medium, which is often referred to as oil. These aggregates have a tendency to solubilize water and other polar species in their core and thus have the potential to function as microreactors.[1] Unlike the reverse micelles formed with ionic surfactants, where well-defined and well-characterized water droplets exist over a wide composition range, the characteristics and constitution of water present in nonionic reverse micelles are not thoroughly understood. This is due to the fact that the headgroups of nonionic surfactants possess long polar chains, which usually get hydrated by the water molecules in a nonionic reverse micelle. Thus, the added water may or may not form a distinct water pool as in the case of reverse micelles formed with ionic surfactants. The nonionic surfactant, Triton X-100 (TX-100), is one such example, and it forms reverse micelles in cyclohexane,[2,3] mixed solvents of benzene−*n*-hexane,[4,5] and in toluene[6,7] under certain conditions. In case of reverse micelles formed with the TX-100 surfactant, the number of water molecules that hydrate the average of 9.5 oxyethylene groups has been found to depend on the nature of the nonpolar solvent.[5]

The structure and the micropolarity of the reverse micelles formed with the TX-100 surfactant in cyclohexane and in solvent mixtures of benzene−*n*-hexane have been thoroughly investigated using light scattering and optical absorption methods by Schelly and co-workers.[2−5] Solvation dynamic studies have also been employed to understand the effect of confinement on the dynamical aspects of these micellar interiors.[8,9] Recently, we have used a fluorescence depolarization method to explore the location and mobility of two structurally similar but chemically distinct hydrophobic probes, 2,5-dimethyl-1,4-dioxo-3,6-diphenylpyrrolo[3,4-*c*]pyrrole (DMDPP) and 1,4-dioxo-3,6-diphenylpyrrolo[3,4-*c*]pyrrole (DPP), solubilized in the TX-100/cylohexane reverse micelles as a function of the water content.[10] It has been observed that the two probes are solubilized in two different regions of the reverse micelle owing to their dissimilar chemical nature. Despite the fact that both the probes are hydrophobic, their mobility is influenced, albeit in a distinct manner, by the addition of water to the TX-100/cylohexane reverse micelles. These findings have been rationalized on the basis of the physical model for these reverse micelles, in which cyclohexane penetrates inside the core, and upon the addition of water the nonpolar solvent is gradually displaced.[2,3] However, the amount of water that can be solubilized in these micelles is not significant. In other words, a maximum value of $W = [H_2O]/[TX\text{-}100]$ that can be reached is only 4.2 at 298 K. The added water does not form a pool in the core of the aggregates, rather it seems to be dispersed between the oxyethylene chains of the surfactant units.[3] The progression of our earlier work[10] in TX-100/cyclohexane reverse micelles has led to another question, namely, how will the microenvironment of these hydrophobic probes be affected when the water droplet formation takes place in nonionic reverse micelles? An attempt to find an answer to this question is the motive for the present study.

In this context, we wish to extend our earlier work[10] to reverse micelles formed in TX-100/benzene−*n*-hexane system with different amounts of added water. This system is structurally very different as compared to the earlier one (TX-100/ cyclo-

* To whom correspondence should be addressed. E-mail: gbdutt@apsara.barc.ernet.in.

10.1021/jp049160d CCC: $27.50
Published on Web 05/06/2004

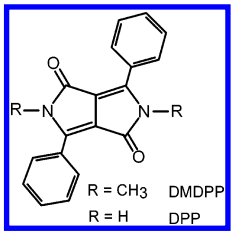

Figure 1. Molecular structures of the probes DMDPP and DPP.

hexane) in the sense that W values as high as 9.0 can be attained when the [TX-100] is 0.27 mol dm^{-3} and the benzene to *n*-hexane ratio is 30:70 (v/v) at 298 K.[4] Moreover, it has also been observed that water droplet formation takes place around $W = 2.5$.[5] As mentioned earlier, our basic interest lies in finding out how the onset of water droplet formation influences the location and mobility of the probes DMDPP and DPP solubilized in these reverse micelles. To accomplish this objective, rotational diffusion of the probes DMDPP and DPP (see Figure 1 for their molecular structures) has been investigated in TX-100/benzene−hexane reverse micellar system with increasing water content using steady-state and time-resolved fluorescence depolarization techniques. We also wish to make a comparison between the relative trends observed in the average reorientation times of DMDPP and DPP in TX-100/benzene−hexane to that in TX-100/cyclohexane as a function of the water content. The outline of the remainder of this paper is organized in the following manner. In section 2, steady-state and time-resolved fluorescence depolarization methods that were used to measure the rotational diffusion of the probes in TX-100/benzene−hexane reverse micelles are briefly described. The results obtained from these measurements are presented in section 3 and are discussed in section 4. The summary of this work is presented in the final section.

2. Experimental Procedures

The probes DMDPP and DPP are from Ciba Specialty Chemicals Inc., Switzerland. The surfactant TX-100, spectroscopic grade benzene, and *n*-hexane are, respectively, from BDH Chemicals Ltd., England; S. D. Fine-Chem Ltd., India; and Sisco Research Laboratories Pvt. Ltd., India. All these chemicals are of the highest available purity and were used as such. Deionized water from Millipore was used in the preparation of the micellar samples. Reverse micelles with desired W values were prepared by weighing appropriate amounts of TX-100 and water in volumetric flasks, and the remaining volumes of the flasks were made up with a 30:70 (v/v) mixture of benzene and hexane. The concentration of TX-100 was kept at 0.27 mol dm^{-3} and that of the probes was maintained in the range of 10^{-5} to 10^{-6} mol dm^{-3}.

Steady-state anisotropies of the samples were measured using a Hitachi F-4010 spectrofluorometer, and the details have been described in our earlier publication.[11] The probes DMDPP and DPP were excited at 440 nm, and the emission was monitored in the range of 515−585 nm. Time-resolved fluorescence measurements were carried out using the time-correlated single-photon counting[12] facility at the Tata Institute of Fundamental Research, Mumbai, and details of the system have been described elsewhere.[13] In brief, the frequency-doubled output of a picosecond Ti:sapphire laser (Tsunami, Spectra Physics) was used as the excitation source, and the probes DMDPP and DPP were excited at 427 nm with a vertically polarized pulse. The decay of the anisotropy, which was created by the preferential excitation, was monitored by measuring the fluorescence decays parallel $I_{\parallel}(t)$ and perpendicular $I_{\perp}(t)$ with respect to the polarization of the excitation source. Fluorescence decays $I(t)$ at the magic angle (54.7°) orientation of the emission polarizer were also collected for the determination of lifetimes. The emission in all three cases was monitored at 550 nm. For the parallel component of the decay, 10 000 peak counts were acquired, and the perpendicular component of the decay was corrected for the *G*-factor of the spectrometer. For all the magic angle decays, a time increment of 80 ps/channel was used, and in case of anisotropy decays, 20 and 40 ps/channel were used, respectively, for micellar samples containing DMDPP and DPP. A total of 512 channels of the multichannel analyzer were employed to collect these decays. Each measurement was performed at least 2−3 times, and the average values are reported. All the measurements were performed at 298 K, and the sample temperature was maintained with the help of a temperature controller, Eurotherm.

TABLE 1: Fluorescence Lifetimes and Anisotropy Decay Parameters of DMDPP in Reverse Micelles of TX-100/ Benzene−Hexane as Function of the Water Content at 298 K

W	τ_f/ns[a]	β	τ_{slow}/ns	τ_{fast}/ns	$\langle\tau_r\rangle$/ns[b]
0.0	6.70	0.15 ± 0.02	0.45 ± 0.08	0.10 ± 0.02	0.15 ± 0.04
1.0	6.87	0.24 ± 0.02	0.62 ± 0.07	0.12 ± 0.01	0.24 ± 0.04
2.0	6.98	0.40 ± 0.07	0.62 ± 0.02	0.15 ± 0.04	0.34 ± 0.07
3.0	7.04	0.39 ± 0.01	0.68 ± 0.04	0.15 ± 0.03	0.36 ± 0.04
4.0	6.97	0.43 ± 0.01	0.73 ± 0.04	0.16 ± 0.05	0.41 ± 0.06
5.0	7.02	0.41 ± 0.04	0.75 ± 0.08	0.15 ± 0.01	0.40 ± 0.06
6.0	7.06	0.46 ± 0.04	0.71 ± 0.01	0.13 ± 0.03	0.40 ± 0.05
7.0	7.03	0.43 ± 0.03	0.71 ± 0.03	0.11 ± 0.01	0.37 ± 0.04
8.0	7.01	0.44 ± 0.02	0.73 ± 0.04	0.12 ± 0.01	0.39 ± 0.04

[a] The maximum error in the fluorescence lifetimes is less than 2%. [b] Calculated using eq 2.

The decays measured in this manner are convoluted with the instrument response function (IRF), which was measured by replacing the sample with a solution that scatters light, and the full-width at half-maximum of the IRF was 40 ps. Lifetimes of the probes DMDPP and DPP in TX-100/benzene−hexane reverse micelles were obtained from the measured fluorescence decays and the instrument response function by an iterative reconvolution method using the Marquardt algorithm as described by Bevington.[14] Likewise, the anisotropy decay parameters were obtained by a simultaneous fit[15,16] of parallel $I_{\parallel}(t)$ and perpendicular $I_{\perp}(t)$ components. The criteria for a good fit were judged by statistical parameters such as the reduced χ^2 being close to unity and the random distribution of the weighted residuals. Details concerning the analysis of the fluorescence and anisotropy decays have been mentioned in our earlier publication;[17] hence, we refrain from further discussion.

3. Results

(A) Fluorescence Lifetimes. Fluorescence decays of DMDPP and DPP in TX-100/benzene−hexane reverse micelles could be adequately described by single-exponential functions with one lifetime at all values of W and are given Tables 1 and 2 for DMDPP and DPP, respectively. There are no significant changes in the lifetimes of both DMDPP and DPP with an increase in the water content, the only exceptions being the lifetimes measured at $W = 0.0$ and 1.0. The fluorescence lifetime serves as an excellent indicator to pinpoint the location of the probe in a multicomponent system like the one used in the present study. The probe DMDPP is soluble in benzene, hexane, mixtures of benzene−hexane, and also in the micellar phase. To find out where exactly DMDPP is solubilized in the TX-100/ benzene−hexane reverse micelles, its fluorescence lifetimes

TABLE 2: Fluorescence Lifetimes and Anisotropy Decay Parameters of DPP in Reverse Micelles of TX-100/ Benzene−Hexane as Function of the Water Content at 298 K

W	τ_f/ns[a]	β	τ_{slow}/ns	τ_{fast}/ns	$\langle\tau_r\rangle$/ns[b]
0.0	5.80	0.49 ± 0.03	1.00 ± 0.05	0.30 ± 0.02	0.64 ± 0.06
1.0	5.99	0.63 ± 0.06	1.44 ± 0.06	0.33 ± 0.07	1.0 ± 0.1
2.0	6.15	0.64 ± 0.01	1.81 ± 0.08	0.54 ± 0.01	1.35 ± 0.07
3.0	6.17	0.63 ± 0.01	1.94 ± 0.04	0.70 ± 0.10	1.48 ± 0.04
4.0	6.14	0.65 ± 0.05	2.09 ± 0.04	0.63 ± 0.08	1.6 ± 0.1
5.0	6.13	0.67 ± 0.02	2.13 ± 0.07	0.70 ± 0.10	1.7 ± 0.1
6.0	6.17	0.69 ± 0.01	2.14 ± 0.03	0.70 ± 0.10	1.69 ± 0.07
7.0	6.16	0.73 ± 0.03	2.21 ± 0.03	0.46 ± 0.05	1.74 ± 0.09
8.0	6.18	0.68 ± 0.03	2.17 ± 0.06	0.56 ± 0.04	1.7 ± 0.1

[a] The maximum error in the fluorescence lifetimes is less than 2%. [b] Calculated using eq 2.

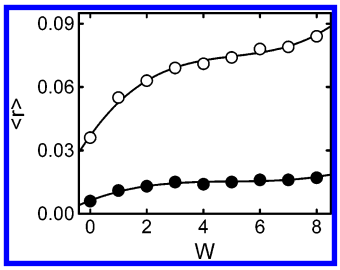

Figure 2. Plots of steady-state anisotropies of DMDPP (●) and DPP (○) in TX-100/benzene−hexane reverse micelles at different values of W. The solid lines through the data points are drawn as a visual aid.

were also measured in benzene, hexane, and a benzene−hexane mixture (30:70 v/v) and have been found to be 6.12, 5.58, and 5.85 ns, respectively. These lifetimes are much shorter than the lifetimes of DMDPP in TX-100/benzene−hexane reverse micelles (see Table 1), which indicates that DMDPP is predominantly solubilized in the micellar phase. DPP, on the other hand, is known to form different kinds of aggregates in the solid state due to intermolecular hydrogen bonding,[18] and the hydrogen bonds between the aggregates need to be broken so that the monomer form of DPP dissolves. As a consequence, it is soluble only in those solvents with which it can form hydrogen bonds. In the case of TX-100, DPP forms hydrogen bonds with the oxyethylene chains and hence is solubilized only in the core of these reverse micelles.

(B) Steady-State Anisotropy. Figure 2 gives plots of steady-state anisotropy $\langle r\rangle$ versus W for both DMDPP and DPP in TX-100/benzene−hexane reverse micelles. It can be observed from the figure that the value of $\langle r\rangle$ increases as the water content in the reverse micelles goes up, but the increase in $\langle r\rangle$ is not uniform. In fact, the value of $\langle r\rangle$ increases by a factor of 2.5 and 1.9, respectively, for DMDPP and DPP, from $W = 0.0$ to 3.0. However, from $W = 3.0$ to 8.0, the increase in $\langle r\rangle$ is almost insignificant for DMDPP and only marginal (about 20%) for DPP. Variation in the steady-state anisotropies as a function of the water content in the reverse micelles can be used to gauge the mobility of the probe molecule if the fluorescence lifetime of a given probe is the same for all values of W. But as was already mentioned, there is some variation in the lifetimes of both DMDPP and DPP at low values of W. In view of this limitation, we resort to time-resolved anisotropy measurements to get a better insight into the location and mobility of the probe molecules in these reverse micelles.

(C) Time-Resolved Anisotropy. Unlike the fluorescence decays, a sum of two exponentials with two time constants was needed to fit the anisotropy decays of both DMDPP and DPP in TX-100/benzene−hexane reverse micelles at all values of

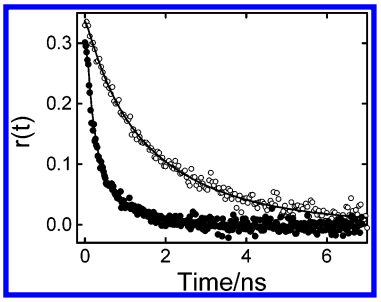

Figure 3. Anisotropy decays of DMDPP (●) and DPP (○) in TX 100/ benzene−hexane reverse micelles at $W = 8.0$. The smooth lines passing through the data points are the fitted ones. The average reorientation times are 0.39 and 1.7 ns, respectively, for DMDPP and DPP.

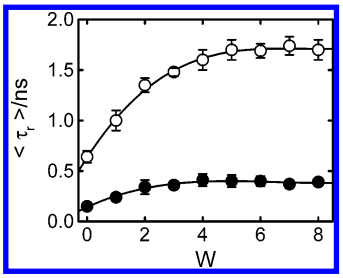

Figure 4. Plots of $\langle\tau_r\rangle$ vs W for DMDPP (●) and DPP (○) in TX 100/benzene−hexane reverse micelles. The solid lines through the experimental points are drawn as a visual aid.

W. The functional form of the time-dependent anisotropy $r(t)$ is given by the following relation:

$$r(t) = r_0[\beta \exp(-t/\tau_{slow}) + (1 - \beta) \exp(-t/\tau_{fast})] \quad (1)$$

In eq 1, τ_{slow} and τ_{fast} are the two time constants associated with the decay of the anisotropy, β is the preexponent that determines the relative contributions of τ_{slow} and τ_{fast} to $r(t)$, and r_0 is the limiting anisotropy. The anisotropy decay parameters for DMDPP and DPP in TX-100/benzene−hexane reverse micelles obtained from the analysis are given in Tables 1 and 2, respectively, together with the average reorientation time $\langle\tau_r\rangle$. The average reorientation time, which is a model independent parameter, is obtained by the following equation:

$$\langle\tau_r\rangle = \beta\tau_{slow} + (1 - \beta)\tau_{fast} \quad (2)$$

The average reorientation times of DPP are a factor of 4 longer than that of DMDPP in these reverse micelles. Figure 3 gives plots of anisotropy decays of DMDPP and DPP in TX-100/ benzene−hexane reverse micelles at $W = 8.0$ together with the fitted curves. It is obvious from the figure that the anisotropy of DPP decays significantly slower than that of DMDPP in the reverse micelles. In an attempt to see how the $\langle\tau_r\rangle$ values of both the probes vary with the water content, they are plotted as a function of W in Figure 4. It can be inferred from Tables 1 and 2 and observed from the figure that $\langle\tau_r\rangle$ for both the probes increases by more than a factor of 2 from $W = 0.0$ to 3.0 and reaches saturation with a further increase in W. This trend is similar to the one observed in the case of steady-state anisotropies, but unlike $\langle r\rangle$, $\langle\tau_r\rangle$ gives a more direct indication of the mobility of the probe molecules in these reverse micelles.

4. Discussion

The site of solubilization and dynamics of organic probe molecules in complex systems such as micelles and reverse micelles are governed by a number of factors such as the structure of the micelle, water content, and micropolarity. Hence,

it is imperative to have a detailed knowledge and understanding of these micellar properties before one can comprehend where exactly the probe molecules are solubilized and how their mobility is influenced in these molecular assemblies. As briefly mentioned in the Introduction, the reverse micelles formed with TX-100 in a benzene−hexane mixed solvent system have been well-characterized.[4,5] At $W = 0.0$, small reverse micelles with a mean hydrodynamic radius r_h of about 3.7 nm are formed. As water is added to the system, these reverse micelles grow in size, and the r_h remains more or less the same, about 8.6 nm, from $W = 2.0$ to 5.0. With a further increase in the value of W, the increase in r_h is steep, and phase separation occurs at $W = 9.5$. The values of mean hydrodynamic radii of TX-100/benzene−hexane reverse micelles as a function of the water content obtained from literature[4] are given in Table 3. These micelles are characterized by a narrow size distribution (polydispersity < 0.08). From optical absorption studies,[5] it has been deduced that a maximum of 2.5 water molecules are bound to the oxyethylene chain of the TX-100 surfactant unit, and this number is much smaller than that for TX-100 in cyclohexane.[2] The reduction in the number of water molecules in case of TX-100/benzene−hexane reverse micelles is due to the competition between benzene and water for the oxyethylene sites. At low values of W, water is dispersed in the polar core and hydrates the oxyethylene chains of the TX-100, and the formation of a water pool begins when $W = 2.5$.

Having gained a detailed understanding of the structure of TX-100/benzene−hexane reverse micelles from literature,[4,5] we try to interpret the fast and slow rotational reorientation times of DMDPP and DPP obtained from the anisotropy decays and subsequently elucidate the location and mobility of the probe molecules. Numerous experimental studies[10,17,19−26] involving the fluorescence depolarization of organic solutes in micelles and reverse micelles indicate that the observed slow and fast rotational relaxation times are a consequence of the solute molecule, depending on its location, undergoing slow lateral diffusion at or near the interface of the micelles and also a fast wobbling motion in an imaginary cone described by semiangle θ. Both these motions are coupled to the overall rotation of the micelle, and this model is popularly known as the two-step model.[27−30] The experimentally measured slow and fast reorientation times are related to the time constants for lateral diffusion τ_L and wobbling motion τ_W by the following relations, and the underlying assumption involved is that the slow and fast motions are separable.

$$\frac{1}{\tau_{slow}} = \frac{1}{\tau_L} + \frac{1}{\tau_M} \tag{3}$$

$$\frac{1}{\tau_{fast}} = \frac{1}{\tau_W} + \frac{1}{\tau_{slow}} \tag{4}$$

Here, τ_M is the time constant for the overall rotation of the micelle and has been calculated from the Stokes−Einstein−Debye (SED) hydrodynamic theory with stick boundary condition.[31]

$$\tau_M = \frac{4\pi r_h^3 \eta}{3kT} \tag{5}$$

In eq 5, η is the viscosity of the medium in which the rotation of the micelle is taking place, and k and T are the Boltzmann constant and absolute temperature, respectively. Reorientation times calculated for the TX-100/benzene−hexane reverse micelles using eq 5 are given in Table 3. However, it must be noted that the τ_M obtained in this manner gives only a rough estimate on the time scale for the micellar rotation, as the exact shape of these micelles is not known. Because τ_M values are in the microsecond time scale, the contribution of τ_M to the slow and fast processes (eqs 3 and 4), which occur on a nanosecond time scale, is almost negligible. Hence, τ_{slow} essentially represents τ_L.

TABLE 3: Mean Hydrodynamic Radius r_h and τ_M Values of TX-100/Benzene−Hexane Reverse Micelles as Function of the Water Content at 298 K

W	r_h/nm[a]	$\tau_M/\mu s$[b]
0.0	3.7	0.02
1.0	7.0	0.14
2.0	8.6	0.26
3.0	8.6	0.26
4.0	8.5	0.25
5.0	8.5	0.25
6.0	10.1	0.42
7.0	11.1	0.56
8.0	17.0	2.00

[a] r_h values were read from Figure 1 of ref 4. [b] τ_M values were calculated using eq 5.

TABLE 4: Order Parameters, Cone Angles, and Wobbling Diffusion Coefficients for DMDPP and DPP in TX-100/Benzene−Hexane Reverse Micelles Obtained from the Analysis of the Anisotropy Decays

	DMDPP			*DPP*		
W	S	$\theta°$	$D_W \times 10^{-8}/s^{-1}$	S	$\theta°$	$D_W \times 10^{-8}/s^{-1}$
0.0	0.39	59.0	16.3	0.70	38.3	2.62
1.0	0.49	52.5	12.2	0.79	31.5	1.86
2.0	0.63	43.2	6.9	0.80	30.7	0.99
3.0	0.62	43.9	7.3	0.79	31.5	0.73
4.0	0.66	41.1	6.2	0.81	29.8	0.80
5.0	0.64	42.5	7.1	0.82	29.0	0.66
6.0	0.68	39.7	7.5	0.83	28.1	0.62
7.0	0.66	41.1	9.7	0.85	26.3	0.99
8.0	0.66	41.1	8.8	0.82	29.0	0.91

The information pertinent to the wobbling motion is contained in τ_{fast}. According to the wobbling-in-cone model, the probe molecules wobble freely inside a cone of semiangle θ. The relaxation time corresponding to the wobbling motion has been obtained from eq 4. The average micellar structure in the vicinity of the probe is given by the order parameter S, which has been obtained using the relation[29,30]

$$S^2 = \beta \tag{6}$$

The order parameters obtained for DMDPP and DPP in TX-100/benzene−hexane reverse micelles using eq 6 are tabulated in Table 4. It can be observed from the table that the values of S are in the range of 0.40−0.68 and 0.70−0.85 for DMDPP and DPP, respectively. Another noticeable point is that the values of the order parameters for both the probes increase considerably when W is increased from 0.0 to 1.0. The high values of the order parameters are an indication that the probes are experiencing somewhat restricted rotation, which is possible only if they are located in the core of these reverse micelles. It has been well-documented that the oxyethylene chains of the TX-100 surfactant units exist in the form of a random coil or in meander conformation[32] and hence do not allow isotropic rotational diffusion of the probes. From the order parameters, the cone angles have been obtained using the following relation:[27]

$$S^2 = \left[\frac{1}{2}(\cos\theta)(1 + \cos\theta)\right]^2 \tag{7}$$

From the calculated values of τ_W, S, and θ, the diffusion coefficients for wobbling motion D_W have been calculated with the aid of the following relation:[30]

$$D_W = \frac{1}{[(1-S^2)\tau_W]}\left[\frac{\cos^2\theta(1+\cos\theta)^2}{2(\cos\theta-1)}\left\{\ln\left(\frac{(1+\cos\theta)}{2}\right)+\frac{(1-\cos\theta)}{2}\right\}+\frac{(1-\cos\theta)}{24}(6+8\cos\theta-\cos^2\theta-12\cos^3\theta-7\cos^4\theta)\right] \quad (8)$$

The cone angles θ and the diffusion coefficients for wobbling motion D_W are also given in Table 4. Further discussion on these data is superfluous as the central theme of this work is to find out whether the microenvironment of the probes is altered with the onset of water droplet formation in these nonionic reverse micelles, and for this purpose, we revert to the average reorientation times.

First, let us consider the case of DMDPP whose $\langle\tau_r\rangle$ values, as already mentioned in the previous section, increase at low values of W and reach saturation upon further increase in the water content. This observation can be rationalized on the following basis. DMDPP is solubilized in the core of TX-100/benzene−hexane reverse micelles, and as the oxyethylene chains of the polar core become hydrated upon the addition of water, DMDPP being a hydrophobic probe alters its location such that it is not in contact with the water molecules. Hence, there is a change in microenvironment experienced by DMDPP at low values of W, which is reflected in the $\langle\tau_r\rangle$ values. However, once water pool formation takes place, the further addition of water does not change its surroundings, and as a consequence, there is no variation in the observed $\langle\tau_r\rangle$ value. A similar pattern has been observed in the $\langle\tau_r\rangle$ versus W plot (see Figure 4) for DPP as well, but a slightly different rationale is needed to assimilate its behavior. It must be noted that DPP is not only hydrophobic but also insoluble in benzene, which penetrates into the aggregates and partially dehydrates the oxyethylene chains of the reverse micelles.[5] As a result, there is no region in the TX-100/benzene−hexane reverse micelles that is devoid of both water and benzene upon the formation of the water droplet. In view of this prevailing situation, it is reasonable to conclude that DPP is bridging adjacent oxyethylene chains strongly enough such that water molecules cannot replace the probe. Under these circumstances, the plausible scenario at low water content would be a change in the microenvironment surrounding DPP but not its location. However, with the onset of water droplet formation, there is neither a change in its microenvironment nor the location.

From the logic and reasoning presented in the analysis, it is obvious that both DMDPP and DPP are solubilized in the polar core of these reverse micelles. But are they located in the same region of the core, the answer is not affirmative. The average reorientation times of DPP are a factor of 4 or more longer than that of DMDPP in TX-100/benzene−hexane reverse micelles, and it is evident from numerous rotational relaxation studies involving DMDPP and DPP in liquids[11,13,33−37] that the significant differences observed in the rotational behavior of these two probes is due to the strong hydrogen bonding interactions of DPP at the two NH sties with its surroundings. In almost all these systems, DPP has been found to rotate a factor of 1.5−3.0 slower than that of DMDPP, and it has been shown that this factor depends on the solute−solvent interaction strength.[37] The fact that the $\langle\tau_r\rangle$ values of DPP are more than a factor of 4 longer as compared to DMDPP in TX-100/ benzene−hexane reverse micelles is an indication that not only specific interactions between the DPP and the oxyethylene groups but also the relative locations of DMDPP and DPP in the polar cores of these micelles, are responsible for the observed disparities in the average reorientation times. This point has been further substantiated by the significant differences observed in the order parameters of DMDPP and DPP.

At this juncture, it is interesting to compare and contrast the relative trends observed in the average reorientation times of DMDPP and DPP in TX-100/benzene−hexane to that in TX-100/cyclohexane as a function of the water content. In the case of the reverse micelles formed in cyclohexane, there is a steady increase in the $\langle\tau_r\rangle$ values with W for DMDPP. The trends observed for DMDPP are almost the same in both types of reverse micelles (i.e., gradual increase in $\langle\tau_r\rangle$ at low water content). The comparison, however, ends there because water droplet formation does not take place in TX-100/cyclohexane reverse micelles. The relative trends observed in $\langle\tau_r\rangle$ for DPP, on the other hand, appear to be somewhat dissimilar in TX-100 reverse micelles in cyclohexane and benzene−hexane. In reverse micelles formed with cyclohexane, there is almost no change in $\langle\tau_r\rangle$ with an increase in W, and in contrast, the average reorientation times increase till the onset of water droplet formation in TX-100/benzene−hexane reverse micelles. In the former case, DPP is located in a region that is devoid of both cyclohexane and water; however, the latter system is considerably smaller (mean hydrodynamic radii of TX-100/ benzene−hexane system are a factor of 3−4 smaller as compared to TX-100/ cyclohexane system at low values of W), and hence, even small amounts of water can have a profound influence on the microenvironment experienced by the probe molecule.

Conclusions

Nonionic reverse micelles can essentially be used as confined systems for carrying out specific chemical reactions provided a thorough understanding of their properties such as the structure, internal environment, distribution of water, and sites of solubilization of organic solutes is attained. Fluorescence depolarization studies of organic solutes solubilized in them serve as a convenient means to investigate some of the aforementioned properties. As a part of our ongoing efforts to comprehend a few specific issues pertinent to the nonionic reverse micelles formed with the surfactant TX-100 in different organic solvents, the present study has been undertaken, and the important conclusions are as follows. In this work, rotational diffusion of two hydrophobic probes, DMDPP and DPP solubilized in TX-100/benzene−hexane reverse micelles with different amounts of water, has been examined. The anisotropy decay of both the probes at all values of W could be adequately described by a sum of two exponentials with two time constants, which has been ascribed to different kinds of motion experienced by the probe molecule inside the micelles. The important observation, however, has been the saturation of the average reorientation times with increasing W for both the probes with the onset of water droplet formation. This has been rationalized on the basis of both DMDPP and DPP experiencing changes in their respective microenvironments with W until the formation of water pools in these reverse micelles. From the magnitude of the differences in the average reorientation times and also from the differences in the values of the order parameters obtained from the two-step model for DMDPP and DPP, it has been inferred that the probes are located in distinct regions of the micelles.

Acknowledgment. Ms. M. H. Kombrabail of the Tata Institute of Fundamental Research is thanked for her help with time-resolved fluorescence experiments. Dr. P. N. Bajaj and Dr. T. Mukherjee are thanked for their encouragement throughout the course of this work.

References and Notes

(1) Fendler, J. H. *Membrane Mimetic Chemistry*; Wiley-Interscience: New York, 1982.
(2) Zhu, D.-M.; Feng, K.-I.; Schelly, Z. A. *J. Phys. Chem.* **1992**, *96*, 2382.
(3) Zhu, D.-M.; Schelly, Z. A. *Langmuir* **1992**, *8*, 48.
(4) Zhu, D.-M.; Wu, X.; Schelly, Z. A. *Langmuir* **1992**, *8*, 1538.
(5) Zhu, D.-M.; Wu, X.; Schelly, Z. A. *J. Phys. Chem.* **1992**, *96*, 7121.
(6) Almgren, M.; van Stam, J.; Swarup, S.; Löfroth, J.-E. *Langmuir* **1986**, *2*, 432.
(7) Rodríguez, R.; Vargas, S.; Fernández-Velasco, D. A. *J. Colloid Interface Sci.* **1998**, *197*, 21.
(8) Mandal, D.; Datta, A.; Pal, S. K.; Bhattacharyya, K. *J. Phys. Chem. B* **1998**, *102*, 9070.
(9) Pant, D.; Levinger, N. E. *Langmuir* **2000**, *16*, 10123.
(10) Dutt, G. B. *J. Phys. Chem. B* **2004**, *108*, 805.
(11) Dutt, G. B.; Srivatsavoy, V. J. P.; Sapre, A. V. *J. Chem. Phys.* **1999**, *110*, 9623.
(12) O'Connor, D. V.; Phillips, D. *Time-Correlated Single Photon Counting*; Academic Press: London, 1984.
(13) Dutt, G. B.; Srivatsavoy, V. J. P.; Sapre, A. V. *J. Chem. Phys.* **1999**, *111*, 9705.
(14) Bevington, P. R. *Data Reduction and Error Analysis for the Physical Sciences*; McGraw-Hill: New York, 1969.
(15) Cross, A. J.; Fleming, G. R. *Biophys. J.* **1984**, *46*, 45.
(16) Knutson, J. R.; Beechem, J. M.; Brand, L. *Chem. Phys. Lett.* **1983**, *102*, 501.
(17) Dutt, G. B. *J. Phys. Chem. B* **2002**, *106*, 7398.
(18) Adachi, M.; Nakamura, S. *J. Phys. Chem.* **1994**, *98*, 1796.
(19) Quitevis, E. L.; Marcus, A. H.; Fayer, M. D. *J. Phys. Chem.* **1993**, *97*, 5762.
(20) Wittouck, N.; Negri, R. M.; Ameloot, M.; De Schryver, F. C. *J. Am. Chem. Soc.* **1994**, *116*, 10601.
(21) Maiti, N. C.; Krishna, M. M. G.; Britto, P. J.; Periasamy, N. *J. Phys. Chem. B* **1997**, *101*, 11051.
(22) Krishna, M. M. G.; Das, R.; Periasamy, N.; Nityananda, R. *J. Chem. Phys.* **2000**, *112*, 8502.
(23) Dutt, G. B. *J. Phys. Chem. B* **2003**, *107*, 3131.
(24) Dutt, G. B. *J. Phys. Chem. B* **2003**, *107*, 10546.
(25) Dutt, G. B. *J. Phys. Chem. B* **2004**, *108*, 3651.
(26) Kelepouris, L.; Blanchard, G. J. *J. Phys. Chem. B* **2003**, *107*, 1079.
(27) Kinoshita, J.; Kawato, S.; Ikegami, A. *Biophys. J.* **1977**, *20*, 289.
(28) Wang, C. C.; Pecora, R. *J. Chem. Phys.* **1980**, *72*, 5333.
(29) Lipari, G.; Szabo, A. *Biophys. J.* **1980**, *30*, 489.
(30) Lipari, G.; Szabo, A. *J. Am. Chem. Soc.* **1982**, *104*, 4546.
(31) Debye, P. *Polar Molecules*; Dover: New York, 1929.
(32) Robson, R. J.; Dennis, E. A. *J. Phys. Chem.* **1977**, *81*, 1075.
(33) Dutt, G. B.; Krishna, G. R. *J. Chem. Phys.* **2000**, *112*, 4676.
(34) Dutt, G. B. *J. Chem. Phys.* **2000**, *113*, 11154.
(35) Dutt, G. B.; Ghanty, T. K. *J. Chem. Phys.* **2002**, *116*, 6687.
(36) Dutt, G. B.; Ghanty, T. K. *J. Chem. Phys.* **2003**, *118*, 4127.
(37) Dutt, G. B.; Ghanty, T. K. *J. Chem. Phys.* **2003**, *119*, 4768.